

The simulations of charged particle acceleration from gas target at 20 TW SOKOL-P laser with intensity of $5 \cdot 10^{19} \text{ W/cm}^2$

V.A. Lykov^a, G.V. Baidin and D.V. Torshin

Russian Federal Nuclear Center – VNIITF, Snezhinsk, Chelyabinsk Reg. 456770, Russia

Abstract. 2D PIC code simulations have been performed for the optimization of gas jet target parameters to achieve a maximal energy and efficiency of charged particle acceleration in planned experiments at the 20 TW picosecond SOKOL-P laser. These calculations specify an opportunity to obtain energy up to $E_e \sim 200 \text{ MeV}$ and efficiency $\eta_e \sim 10\%$ for accelerated electrons and $E_p \sim 30 - 50 \text{ MeV}$ and $\eta_p \sim 5\%$ for accelerated protons in these experiments at laser intensity $I \sim 5 \cdot 10^{19} \text{ W/cm}^2$. They show the necessity of providing a formation of hydrogen jets with diameter $\sim 1 \text{ mm}$, a gas molecule concentration $\sim 2 \cdot 10^{19} \text{ cm}^{-3}$ and steep density gradients $\sim 200 \mu\text{m}$ at the edge of the gas jet target for achieving these parameters of laser accelerated particle beams.

1. INTRODUCTION

The experimental and theoretical studies of charged particle acceleration by ultra-short high-intensity laser pulses attract interest in view of possible applications in science and engineering [1–3].

The SOKOL-P laser with energy $E \approx 15 \text{ J}$ and pulse duration $\tau \sim 0.7 \text{ ps}$ operates at RFNC-VNIITF. The achieved laser pulse contrast made it possible to study proton generation by irradiation of a thin foil using a pulses with intensity $I \sim 10^{19} \text{ W/cm}^2$ [4]. The fast electron temperature $T_H \sim 1 \text{ MeV}$ and fast protons energy up to $E_{p,\text{max}} \sim 10 \text{ MeV}$ have been measured in these experiments. The main mechanism of proton acceleration in SOKOL-P experiments was TNSA. It is known that for efficient proton acceleration at TNSA regime, the plasma profile near the rear side of the target must be steep before the main laser pulse come on target. It imposes rigid requirements to laser pulse contrast. The requirements to contrast of laser pulse could be less rigorous if gas jet is used as targets in experiments on laser particle acceleration. The effective electron temperature is higher in experiments on the irradiation of gas jets [5, 6] and low density foams [7] by picosecond laser pulses than in experiment with solid state target, therefore it was possible to expect an increase in the maximum energy of ions using low-density targets. 2D PIC code simulations of ion acceleration at the irradiation of a low-density target by relativistic laser pulses were already published [5–7]. However these simulations were executed for laser parameters differing from SOKOL-P laser.

Below are presented results of 2D PIC simulations performed using the *LegoLPI* [8] and *Mandor* [9] codes to find the optimal parameters of gas jet for efficient charged particles acceleration in forthcoming experiments at SOKOL-P laser. The use of two different PIC codes raises reliability of simulation.

^ae-mail: v.a.lykov@vniitf.ru

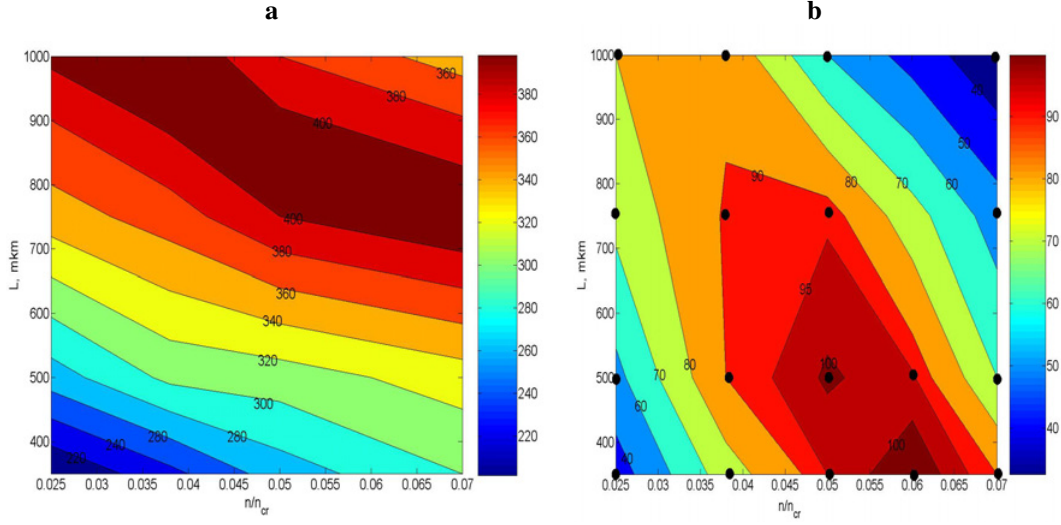


Figure 1. (a) Maximum electron energy (MeV) at time $t_1 = L/c + t_0$ versus target parameters L and n_e/n_{cr} and (b) maximum proton energy (MeV) at time $t_2 = L/c + 2t_0$ versus target parameters L and n_e/n_{cr} .

2. THE OPTIMIZATION OF GAS TARGET PARAMETERS BY 2D PIC CODES

The 2D Mandor simulations were fulfilled for condition of the 20 TW picosecond laser pulse irradiation of a homogeneous hydrogen jets with variation of jet's length and density.

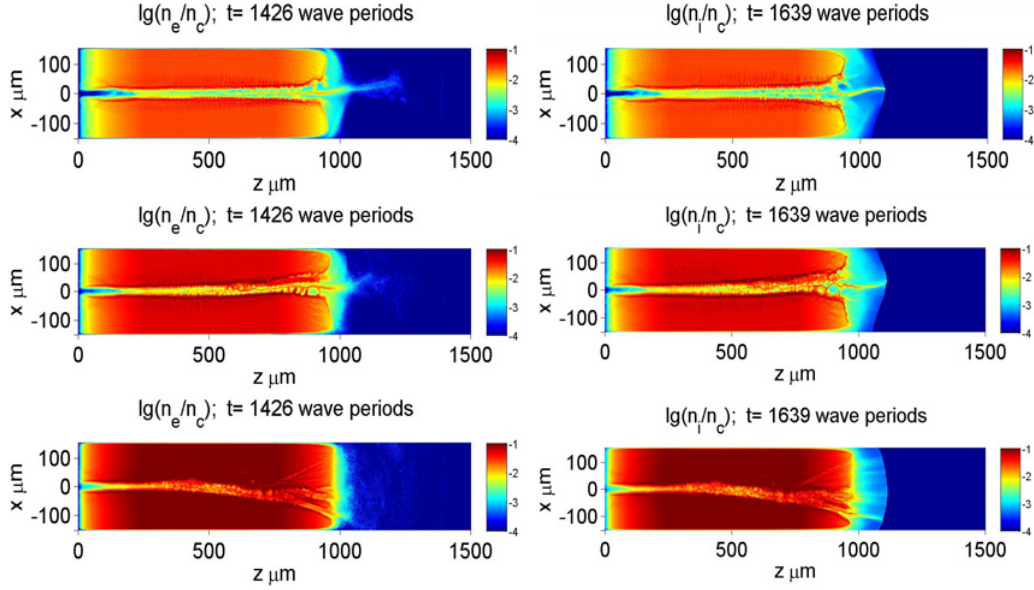
The laser pulse with $\lambda = 1.0 \mu\text{m}$ and peak intensity $I_{max} = 5 \cdot 10^{19} \text{ W/cm}^2$ falls normally at hydrogen layer. The pulse has Gauss profile both in longitudinal and transversal directions with $T_{FWHM} = 0.7 \text{ ps}$ and $D_{FWHM} = 6 \mu\text{m}$. The intensity has maximum at time $t_0 = T_{FWHM}$. The laser light polarization is of linear type with electric field in the simulation plane (p-polarization). The initial plasma density (n_e) and length (L) are varied in a wide range: $350 < L (\mu\text{m}) < 1000$ and $0.025 < n_e/n_{cr} < 0.07$, where $n_{cr} = m_e \omega^2 / 4\pi e^2$, where m_e and e - electron mass and charge, ω - laser frequency. The calculation box is $L + 500 \mu\text{m}$ in longitudinal and $500 \mu\text{m}$ in transversal directions. Cell size is $0.1 \mu\text{m} \times 0.1 \mu\text{m}$. Targets with thickness $L < 350 \mu\text{m}$ were not examined in view of problems with gas-jet realization with such parameters in practice.

The electron energy cutoff obtained in these calculations is presented in Figure 1a at time when the pulse intensity maximum is leaving the target rear side: $t_1 = L/c + t_0$. It could be seen from Figure 1a that electron energy reaches 200-400 MeV and it has weak dependence from density, but rises with target width L . The calculated proton energy cutoff is compared in Figure 1b at time when pulse tail is leaving the rear target side: $t_2 = L/c + 2t_0$. Figure 1b points to a wide range of target lengths and densities where proton energy reaches 80-100 MeV for targets with $n_e = (0.03 - 0.06) \cdot n_{cr}$ near a curve $L \sim (n_e)^{-1.7}$. The efficiency of laser energy transfer to charged particles is almost constant and has a value of 20% along this curve also according to performed calculations.

The 2D Mandor code calculations performed for triangular and trapezoid initial density plasma profile keeping constant the mean electron density and total target mass ($L \cdot n_e = const$) show that density gradient at the target borders has a weak influence on electron spectrum but strong influence on proton spectrum. The most significant role for maximal proton energy is played by the density gradient at the target rear side. For example, in the calculation with $250 \mu\text{m}$ length of density gradient at rear side of the target, the maximum of proton energy is 1.5 times smaller as compared with simulation performed for rectangular density profile ($n_e = 0.05 n_{cr}$, $L = 500 \mu\text{m}$). The use of a target with a density profile

Table 1. The results of 2D- *LegoLPI* code calculations for profiled hydrogen jet.

Initial density, $\delta = n_{max}/n_{cr}$	0.0125	0.025	0.050	0.10
Maximal electron energy at $t_1 = L/c + t_0$, (MeV)	362	388	574	264
Maximal proton energy at $t_2 = L/c + 2t_0$, (MeV)	48	64	68	62
Electron efficiency, (%)	11	16	34	67
Proton efficiency, (%)	3	7	14	21

**Figure 2.** The distributions of electron concentrations at the time $t_1 = L/c + t_0$ (left) and proton concentrations at time $t_1 = L/c + 2t_0$ (right) for trapezoid profile of initial density with $\delta = 0.025; 0.05; 0.10$ (from top to down).

in form of isosceles triangle with base $L = 1000 \mu\text{m}$ decreases the maximum of proton energy 5 times compared with target with rectangular density profile.

The target optimization results were specified in a series of 2D *LegoLPI* code calculations. The laser pulse parameters are as mentioned above. The target is an ionized hydrogen layer with initial trapezoid density profile in the longitudinal direction: the concentration $n_e(z)$ was increased from 0 to n_{max} over a distance $z = 2 \dots 252 \mu\text{m}$, it was constant over $z = 252 \dots 752 \mu\text{m}$ and then n_e was decreased to 0 over a distance $z = 752 \dots 1002 \mu\text{m}$. The ratio $\delta = n_{max}/n_{cr}$ was varied in a range: $\delta = \{0.0125; 0.025; 0.05; 0.1\}$.

The results of 2D *LegoLPI* calculations performed with calculation box $1500 \times 307 \mu\text{m} \times \mu\text{m}$, square cell size of $0.075 \mu\text{m}$ and time step of 0.075fs are presented in Table, Figures 2 and Figure 3.

Table and Figure 2 demonstrate different cases of plasma channel formation and particle acceleration in dependence of initial plasma concentration for constant jet length of 1 mm. The gradual increase of plasma concentration leads to improvement of energy transfer from laser pulse to electrons. But starting with some value of plasma mass ($L \cdot n_e$), the laser energy ($\sim 10 \text{J}$) turns out to be insufficient for channel formation at total target length. Besides, filamentation, hosing and other plasma instabilities [10] occur that destroy the straightforwardness of the plasma channel and deflect accelerated particles beam from initial laser direction. According to theory [11] applied for the examined parameters of laser pulse, a high-quality plasma channel could be expected for $n_e < 0.06n_{cr}$ that one could see from our calculations also.

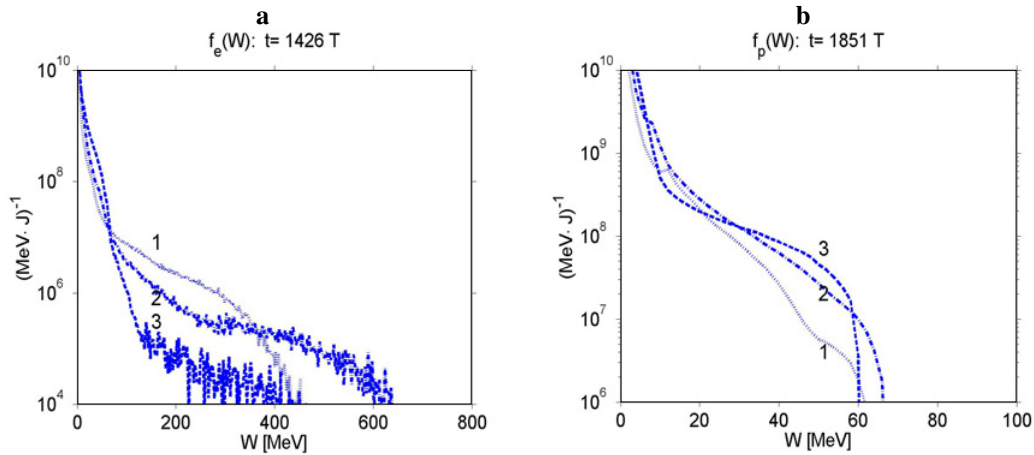


Figure 3. (a) Electron spectra (normalized to laser energy) at the time $t_1 = L/c + t_0 = 4.75$ ps for trapezoidal profile of initial density: 1 – $\delta = 0.025$, 2 – $\delta = 0.05$ and 3 – $\delta = 0.10$; (b) Proton spectra (normalized to laser energy) at the time $t_2 = L/c + 2t_0 = 6.1$ ps for the same density profiles.

According to performed 2D PIC simulations the optimal gas target for SOKOL-P experiments with laser intensity $\sim 5 \cdot 10^{19} \text{ W/cm}^2$ could be a gas jet with diameter ~ 1 mm, density gradient length $\sim 250 \mu\text{m}$ and hydrogen molecules concentration $\sim 2 \cdot 10^{19} \text{ cm}^{-3}$ at jet axis.

The generation of electron beams with energy up to 400 MeV and proton beams with energy up to 60 MeV with efficiency $\sim 10\%$ was observed in performed simulations (see Table and Figure 3). However, in view of possible 3D effects it is more realistic to expect generation of electrons with energy up to 100–200 MeV and protons with energy up to 30–50 MeV in experiments with gas-jet that are planned at 20 TW SOKOL-P laser.

The authors thank D.V. Romanov for Mandor code development, A.V. Brantov and V.Yu. Bychenkov for discussions, S.Yu. Mokshin and E.M. Romanova for program maintenance.

References

- [1] G.A. Mourou, T. Tajima, S.V. Bulanov, *Rev. Mod. Phys.* **78**, 309 (2006)
- [2] A. Pukhov, *Rep. Prog. Phys.* **66**, 47 (2003)
- [3] K.W.D. Ledingham, W. Galster, *New Journal of Physics* **12**, 045005 (2010)
- [4] K.V. Safronov, D.A. Vikhlyaev, A.G. Vladimirov, D.S. Gavrilov, S.A. Gorokhov, A.G. Kakshin, E.A. Loboda, V.A. Lykov, E.S. Mokiecheva, A.V. Potapov, V.A. Pronin, V.N. Saprykin, P.A. Tolstoukhov, O.V. Chefonov, M.N. Chizhkov, *JETP Lett.* **88**, 716 (2008)
- [5] B.R. Walton, S.P.D. Mangles, Z. Najmudin, M. Tatarakis, M.S. Wei, A. Gopal, C. Marle, A.E. Dangor, K. Krushelnick, S. Fritzler, V. Malka, R.J. Clarke, C. Hernandez-Gomez, *Phys. Plasmas* **13**, 113103 (2006)
- [6] L. Willingale, S.P.D. Mangles, P.M. Nilson, R.J. Clarke, A.E. Dangor, M.C. Kaluza, S. Karsch, K.L. Lancaster, W.B. Mori, Z. Najmudin, J. Schreiber, A.G. R. Thomas, M.S. Wei, K. Krushelnick, *Phys. Rev. Lett.* **96**, 245002 (2006)

- [7] L.Willingale, S. R. Nagel, A.G.R. Thomas, C.Bellei, R.J. Clarke, A.E. Dangor, R.Heathcote, M.C. Kaluza, C. Kamperidis, S. Kneip, K. Krushelnick, N. Lopes, S.P.D. Mangles, W. Nazarov, P.M. Nilson, Z. Najmudin, *Phys. Rev. Lett.* **102**, 125002 (2009)
- [8] G.V.Baidin and V.A.Lykov, *Journal of Physics: Conference Series* **244**, 022046, (2010)
- [9] D.V.Romanov, V.Yu.Bychenkov, W.Rozmus, C.E. Capjack, R. Fedosejevs, *Phys. Rev. Lett.* **93**, 215004 (2004)
- [10] E. Esarey, C.B. Schroeder, W.P. Leemans, *Rev. Mod. Phys.* **81**, 1229 (2009)
- [11] A. Friou, E. Lefebvre, and L. Gremillet, *Phys. Plasmas* **19**, 022704 (2012)